Article
Chinese Science Bulletin
Plant Physiology
May 2012 Vol.57 No.15: 1803–1809
doi: 10.1007/s11434-011-4937-6

Molecular studies of the *Medicago truncatula MtAnn3* gene involved in root hair deformation

GONG ZiYing[1†], SONG Xue[2†], CHEN GongYou[2], ZHU JiaBi[1], YU GuanQiao[1] & ZOU HuaSong[2*]

[1] *National Laboratory of Plant Molecular Genetics, Shanghai Institute of Plant Physiology and Ecology, Shanghai Institutes for Biological Science, Chinese Academy of Sciences, Shanghai 200032, China;*
[2] *School of Agriculture and Biology, Shanghai Jiao Tong University, Shanghai 200240, China*

Received August 8, 2011; accepted October 8, 2011; published online February 23, 2012

The full-length annexin gene, *MtAnn3*, of *Medicago truncatula* was cloned by 5′ RACE. Compared with typical annexins, which contain a head domain and four homologous repeats in the conserved core domain, the MtAnn3 protein has only one repeat in the core domain. MtAnn3 can bind cell membranes when transiently expressed in onion epidermal cells. *Agrobacterium rhizogenes*-mediated transformation of *MtAnn3* into *Medicago* roots revealed that overexpression of the gene can change the polarity of root hair growth in Ca^{2+}-free medium. The plant hormone cytokinin was able to upregulate the expression of *MtAnn3*. While *MtAnn3* transcripts were detected in young nodules, expression was not nodule-specific, and could be detected at high levels in the roots, stems and leaves as well.

***Medicago truncatula*, *MtAnn3*, annexin, root hair deformation**

Citation: Gong Z Y, Song X, Chen G Y, et al. Molecular studies of the *Medicago truncatula MtAnn3* gene involved in root hair deformation. Chin Sci Bull, 2012, 57: 1803–1809, doi: 10.1007/s11434-011-4937-6

The growth of plant root hairs is a highly polarized process, with Ca^{2+} playing a crucial role. In fact, during root hair growth, the concentration of cytoplasmic Ca^{2+} at the tip region is 10-fold higher than that in the rest of the cell [1], and blocking Ca^{2+} channel activity disrupts root hair growth [2]. In response to the Nod factors secreted by rhizobia, *M. truncatula* root hairs exhibit a rapid and transient plasma membrane depolarization [3]. Subsequently, oscillations in the cytosolic Ca^{2+} concentration, known as Ca^{2+} spiking, are induced. Legume plants undergo several physiological reactions, including root hair curling, which results in the production of new organs called nodules [4].

Annexins are a family of structurally related proteins characterized by the ability to bind phospholipids in a Ca^{2+}-dependent manner [5]. They have an evolutionarily conserved structure with an approximate 70 amino acid motif that is repeated 4 times, and they also contain a discrete calcium-binding site. Each annexin is composed of two principal domains: a divergent N-terminal head and a conserved C-terminal protein core. The latter harbors the Ca^{2+} and membrane-binding sites, and mediates membrane binding [6]. The *Medicago truncatula MtAnn1* gene is transcriptionally activated in root tissues in response to Nod factors. Studies using MtAnn1-GFP reporter fusions have revealed that MtAnn1 is a cytosolic protein localized to the nuclear periphery in cortical cells activated during the early stages of nodulation [7]. A homologous gene, *MtAnn2*, is active in nodule primordia during the early stages of nodulation. In mature nodules, *MtAnn2* expression is confined to the nodule vasculature [8].

As a positive regulator of nitrogen-fixation, the *Sinorhizobium meliloti nifA* gene exerts pleiotropic effects in nodulation [9]. Mutations in *nifA* produce large-scale alterations in gene expression in *S. meliloti* [10,11]. There are functional differences between *nifA* genes from different species.

†These authors contributed equally to this work.
*Corresponding author (email: hszou@sjtu.edu.cn)

For example, certain functional alterations, particularly in the symbiotic phenotype, cannot be restored by the *Bradyrhizobium japonicum* or the *Mesorhizobium huakuii nifA* genes [12]. cDNA-AFLP analysis revealed that the expression of a variety of host genes are altered in *nifA* mutant nodules. One fragment, corresponding to an annexin gene, *MtAnn3*, was upregulated [13]. In this work, we examine the expression and function of *MtAnn3* in detail. Our results provide novel insight into the role of annexins in plants.

1 Materials and methods

1.1 Plants, bacteria and plasmids

Medicago truncatula cv. Jemalong (line A17) was used for all of the experiments. *Agrobacterium* strain MSU440, containing the pRi plasmid, pRiA4, was used to transform *Medicago*. The plasmid pA7-GFP was used for transient expression of GFP fusion proteins in onion epidermal cells.

1.2 5′ RACE

Isolation of total RNA was performed as previously described [13]. Full-length cDNA was obtained by RNA ligase-mediated rapid amplification of cDNA ends using the 5′ RACE System for Rapid Amplification of cDNA Ends (Version 2.0, Invitrogen, USA), according to the manufacturer's instructions. One pair of nested PCR primers was designed: GSP1, 5′-TAGATACAGAATCATGGAA-3′ and GSP2, 5′-TGGAAACTGGAGGAATTAGAAT-3′. The full-length cDNA sequence was used to design forward and reverse gene-specific primers to amplify the open reading frame.

1.3 RT-PCR

The primers for detecting the *MtAnn3* transcript in *Medicago* roots were 5′-CCGGAACTCCCGGTTACATG-3′ and 5′-ACCTCCAGACATATGTGACA-3′. As a control for the concentration and quality of the RNA template, an additional RT-PCR was performed under the same conditions with primers based on the sequence of the *MtActin2* gene (5′-TGGCATCACTCAGTACCTTTCAACAG-3′ and 5′-ACCCAAAGCATCAAATAATAAGTCAACC-3′). The parameters for PCR were as follows: 94°C for 5 min, followed by 28 cycles at 94°C for 50 s, 53°C for 40 s and 72°C for 50 s, and terminated at 72°C for 10 min.

1.4 Subcelluar localization

The complete and C-terminal-truncated MtAnn3 were PCR-amplified using primer 5′-GCTCTAGAGATGAGCTACTACGATCATCAACAAC3′ combined with 5′-CGGGATCCTAAAAGCAAGCATCCAGCATGCAA-3′ or 5′-CGGGATCCTCAAACTTCTTTGTTCTGCTGAGGCTGT-3′, respectively. The 2 PCR fragments were digested with *Xba* I and *Bam*H I and separately cloned into pA7-GFP, generating GFP fusion proteins. The latter generated a C-terminal truncated MtAnn3 with a 21-amino acid deletion. Onion epidermal cells were bombarded with a particle gun-mediated gene delivery system (Bio-Rad, USA). The bombarded onions were incubated in darkness for 24 h before visualization of transient expression using a confocal laser-scanning microscope (Carl Zeiss LSM 510) with a standard filter set.

1.5 Construction of plasmids for transformation

To generate an overexpression construct, the full-length cDNA was amplified by RT-PCR with primers 5′-TGGGCGCGCCTCATAATCACTTTTCAGTTTCATCA3′ and 5′-CGGGGATCCAGAACTAAAAGCAAGCAT-3′. *Asc* I and *Bam*H I sites were introduced at the 5′ ends of the forward and reverse primers, respectively. The PCR product was ligated into the pRNAi plasmid [14]. After digestion with *Hin*d III, the 1.8-kb DNA fragment containing the full-length cDNA and the 35S promoter was inserted into the *Hin*d III-treated binary vector pCAMBIA1301.

A BLAST search in GenBank revealed that the full cDNA sequence was identical to that of a *Medicago* genomic clone (AC140720.21). This genomic sequence information was used to design a pair of primers: 5′-CGAGCTCGATATGAAAATTATGAACATAGGGAG-3′ and 5′-CGAGCTCTGGAACACCAACAGGAGGTTGT-3′. A *Sac* I site was introduced at the 5′ end of the forward and reverse primers. Using genomic DNA as the template, the primers were used to amplify a 1.8-kb sequence upstream of the *MtAnn3* gene. The PCR product was cloned into the pGEM-T vector (Promega, USA) and subsequently transferred into the binary vector pCAMBIA1301-POG.

1.6 *Agrobacterium* rhizogene-mediated transformation

For surface-sterilization, *Medicago* seeds were soaked for 5 min in 70% alcohol, washed 3 times in sterile water, and then treated for 10 min with 30% hypochlorite (commercial bleach). They were subsequently rinsed 10 times in sterile water and plated onto Färhaeus media (0.9 mmol L^{-1} $CaCl_2$, 0.8 mmol L^{-1} Na_2HPO_4, 0.7 mmol L^{-1} KH_2PO_4, 0.5 mmol L^{-1} $MgSO_4$, 0.5 mmol L^{-1} NH_4NO_3, 20 μmol L^{-1} ferric citrate, 100 μg L^{-1} $MnCl_2$, 100 μg L^{-1} $CuSO_4$, 100 μg L^{-1} $ZnCl_2$, 100 μg L^{-1} H_3BO_3 and 100 μg L^{-1} Na_2MoO_4, pH 7.4). Seeds were vernalized for 1 d at 4°C and germinated at 28°C for 24 h in the dark. One-day-old seedlings were then transferred onto new 11-cm Färhaeus media plates at an average density of 5 seedlings per plate. The plates were then placed at 21°C (16 h/8 h light/dark cycle) after removing the seed coat. After approximately 30 h of germination, the seedlings were expected to have a radicle length of approximately 1 cm. The seedlings were placed in a glass Petri dish containing water to avoid desiccation of the radicle.

The hypocotyl was cut approximately 3 mm from the root tip with a sterile scalpel. The wound surface was then inoculated with *Agrobacterium* MSU440 containing the appropriate binary plasmid. The seedlings were co-cultivated with *Agrobacterium* for 5 d at 21°C (16 h/8 h light/darkness) and subsequently transferred to the Emergence medium as described previously [14].

For histochemical β-glucuronidase (GUS) staining, the root fragments and nodules were excised from the plant and prefixed by vacuum infiltration with an ice-cold solution of 0.3% formaldehyde in 0.1 mol L^{-1} potassium phosphate buffer, pH 7.0, followed by incubation on ice for 45 min. After 2 washes in phosphate buffer, the tissues were immersed in the GUS substrate solution in the dark at 37°C for 2–4 h. After rinsing in phosphate buffer, the stained tissues were briefly cleared with sodium hypochlorite (2 min) and rinsed with water. The root fragments and nodules were then removed on microscopic slides, cleared for 1–3 h with a few drops of Hoyer's solution (7.5 g gum arabic, 100 g chloral hydrate and 5 mL glycerol, in 30-mL water), and observed under a microscope (Leica DME, Germany).

1.7 Phytohormone treatment

The transgenic plants with the *MtAnn3* promoter-GUS fusion were transferred to new Färhaeus plates. Sterile filter paper was placed onto each plate to cover the hairy roots. For every plate, 500 μL of a 5 or 10 μmol L^{-1} solution of 6-BA was added to the filter paper. After incubation for 1 d, the hairy roots were used for GUS staining to detect promoter activity.

1.8 Northern blot

Total RNA was isolated using the RNAgents total RNA isolation system (Promega, America). Total RNA (20 μg/lane) was separated by formaldehyde gel electrophoresis. The *MtAnn3* DNA fragment amplified by RT-PCR was used as the hybridization probe, which was labeled using the PCR DIG Probe Synthesis Kit (Roche AB, Sweden). Following hybridization and washing, autoradiography was performed according to manufacturer's suggestion (Roche AB, Sweden).

2 Results

2.1 Full-length *MtAnn3*

The upregulated mRNA fragment in *S. meliloti nifA* mutant nodules (GenBank, DR159687) shared 100% identity with an *M. truncatula* cDNA sequence present in GenBank (EV260869). This cDNA sequence was 658 bp, with a poly(A) tail. RNA ligase-mediated rapid amplification of cDNA ends was used to determine the 5′ end of this cDNA. The result demonstrated that the entire 5′ sequence was present in the 658-bp cDNA. Thus, the full-length cDNA contained a 276-bp open reading frame, a 161-bp 5′ untranslated region, and a 221-bp 3′ untranslated region. Because the open reading frame was identical to the N-terminal sequence of annexins, this gene was designated *MtAnn3*. The predicted MtAnn3 protein was 92 amino acids with 4 YPP and six PQQ repeats. A myristoylation motif was found in the C-terminal region. MtAnn3 shares 26%–98% identity with its homologues in *Arabidopsis thaliana, Zea mays* and *Oryza sativa* (Figure 1).

2.2 Subcellular localization of MtAnn3 in the plant cell

To determine whether MtAnn3 was localized to the cell membrane, we constructed an MtAnn3-GFP fusion protein in the pA7-GFP vector. Confocal imaging of GFP fluorescence revealed that the MtAnn3-GFP fusion protein was localized in the cytoplasmic membrane, as well as in the cytoplasm. The MtAnn3-GFP fusion protein could not be detected in the nucleus (Figure 2(a) and (b)). In contrast, the green fluorescence of the GFP control was observed throughout the plasma membrane, cytoplasm and nucleus

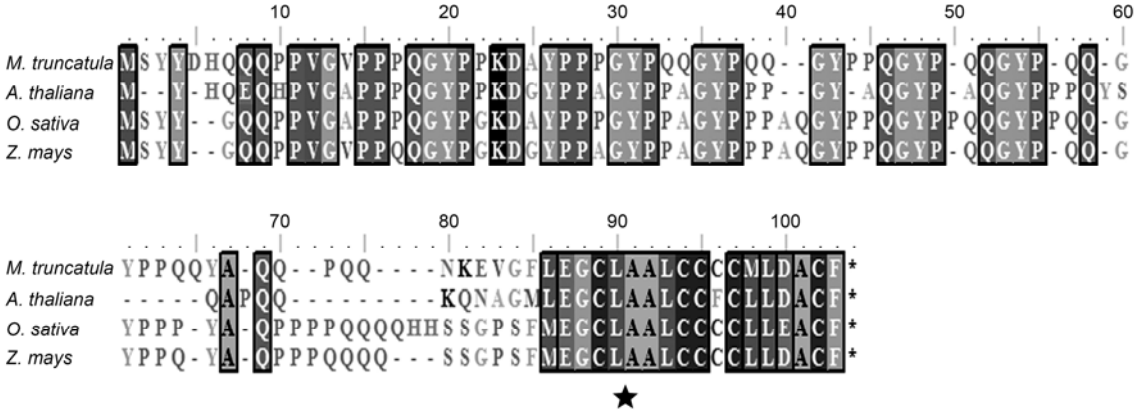

Figure 1 Amino acid sequence alignments of MtAnn3 with selected homologs from *Zea mays*, *Oryza sativa* and *Arabidopsis thaliana*. The putative myristoylation motif at the C-terminus is conserved and is indicated by a star.

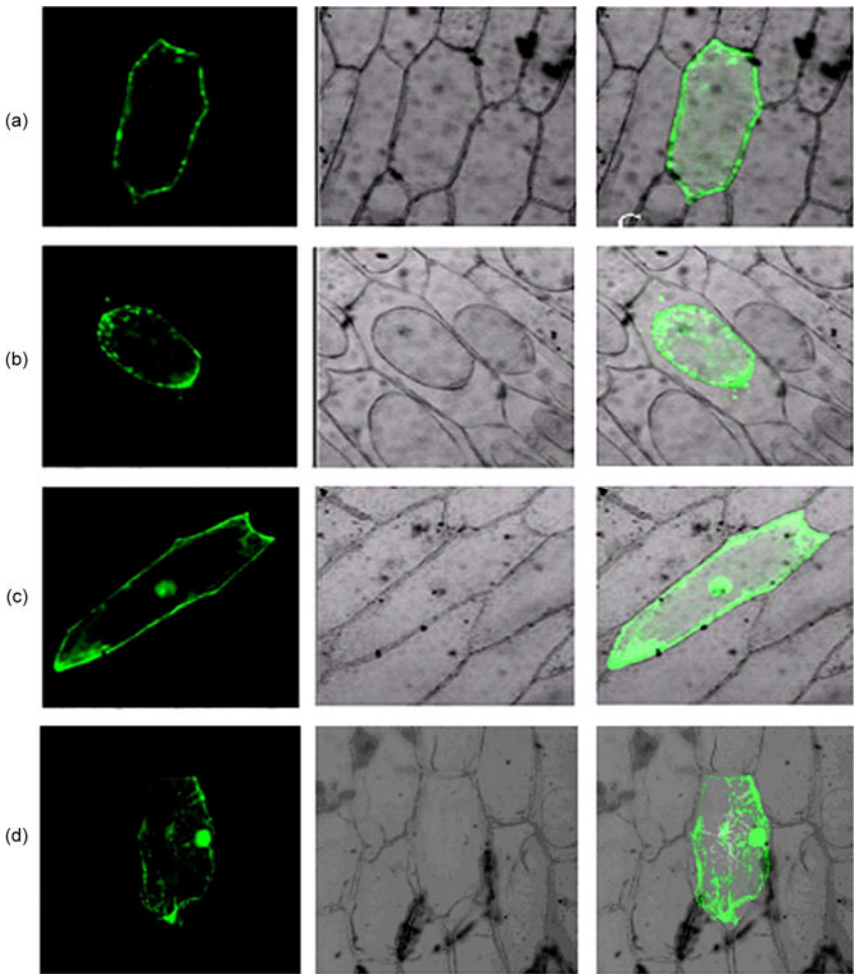

Figure 2 Subcellular localization of MtAnn3. (a) MtAnn3-GFP fusion; (b) MtAnn3-GFP fusion after plasmolysis; (c) empty vector control; (d) C-terminus deletion MtAnn3-GFP fusion.

(Figure 2(d)). It was unexpected that the cytoplasmic membrane was not the sole site of localization, as some fusion protein could be detected in the cytoplasm. In the cells expressing $MtAnn3_{1-72}$, with a 21-amino acid deletion comprising the myristoylation motif, fluorescence was observed throughout the whole cell, including the nucleus, similar to the GFP control (Figure 2(c)), indicating that the myristoylation site is essential for specific subcellular localization of MtAnn3 in plant cells.

2.3 Overexpression of *MtAnn3* results in root hair deformation

To examine the role of *MtAnn3* in plant growth, *Medicago* plants were transformed with an overexpression construct driven by the 35S promoter in the pCAMBIA1301 vector. We used *A. rhizogene*-mediated transformation to generate transgenic plant roots. After 10 d of growth under kanamycin selection, the composite plant hairy roots were used in GUS staining experiments. RT-PCR analysis indicated that *MtAnn3* expression was effectively increased in the hairy roots containing the overexpression construct (Figure 3 (a)).

Based on the fact that *MtAnn3* is an annexin gene and its function should be modulated by calcium, we first grew the transformed roots in Färhaeus medium for 2 weeks until the hairy roots were well developed. The roots harboring the *MtAnn3* overexpression construct showed no difference relative to the roots harboring the empty vector control. Then, the transgenic plants were transferred to Färhaeus media without $CaCl_2$. Under Ca^{2+}-free growth conditions, the root hair tips, harboring the *MtAnn3* overexpression construct, changed their morphologies from elongating to swelling, and branching root hairs were occasionally observed (Figure 3(b)). We counted 20 plants from 4 repeat experiments. In total, 1464 root hairs were scored, and 440 were deformed, for an average deformation ratio of 30%.

2.4 Expression pattern of *MtAnn3*

The *MtAnn3* promoter-GUS fusion was constructed to follow *MtAnn3* gene expression during the steps of nodule initiation and development. As the transformed roots were

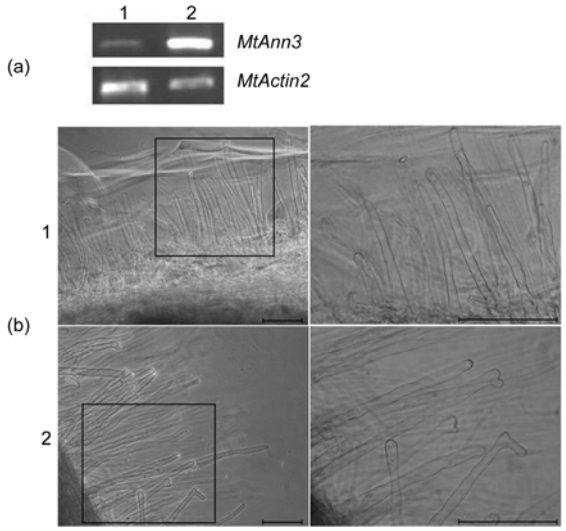

Figure 3 *MtAnn3* overexpression leads to root hair deformation. (a) RT-PCR detection of *MtAnn3* expression in roots containing the overexpression construct; (b) deformed root hairs caused by *MtAnn3* overexpression. The bar indicates 100 μm. 1, empty vector control; 2, *MtAnn3*-overexpressing plant root.

well developed, *S. meliloti* Rm1021 was inoculated onto the hairy roots. The *MtAnn3* promoter was strongly activated at 4 days post inoculation as the nodule primordia formed. Subsequently, *MtAnn3* promoter activity was examined every 2 d. In nodules older than 16 d, GUS activity gradually decreased. In 26-day-old nodules, no GUS activity was observed (Figure 4 (a)). To determine whether *MtAnn3* expression was nodule-specific, a Northern blot was performed on RNA from the nodules, roots, stems and leaves of plants infected with *S. meliloti* Rm1021. The results in Figure 4(b) demonstrate that *MtAnn3* is expressed in all tissues examined. Thus, it is not a nodule-specific gene.

2.5 *MtAnn3* is induced by cytokinin

We also studied the effects of the cytokinin, 6-BA, on *MtAnn3* expression. In transformed roots, the GUS reporter gene, under the control of the *MtAnn3* promoter, was constitutively expressed in the vasculature. After applying 5 μmol L^{-1} 6-BA, GUS activity showed no difference from the untreated control. When the concentration of 6-BA was increased to 10 μmol L^{-1}, GUS activity was observed in all of the root tissues, indicating that *MtAnn3* expression is induced by 6-BA (Figure 5).

3 Discussion

Annexins are composed of two principal domains: a divergent N-terminal head and a conserved C-terminal protein core. The conserved C-terminal domain shares a characteristic peptide sequence of 70 amino acids, which is repeated

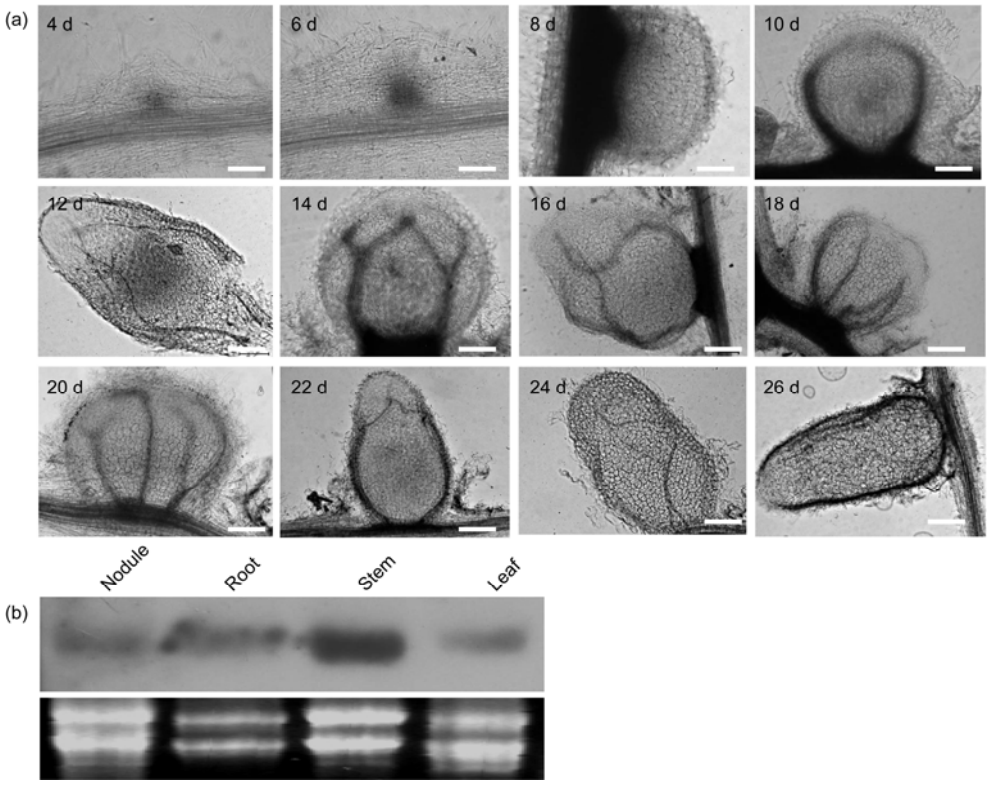

Figure 4 Expression pattern of *MtAnn3*. (a) Promoter-directed GUS activity in nodules; (b) Northern blot analysis of *MtAnn3* expression in nodule, root, stem and leaf. The lower panel shows the electropherogram of methanol denaturing gel electrophoresis of total RNA.

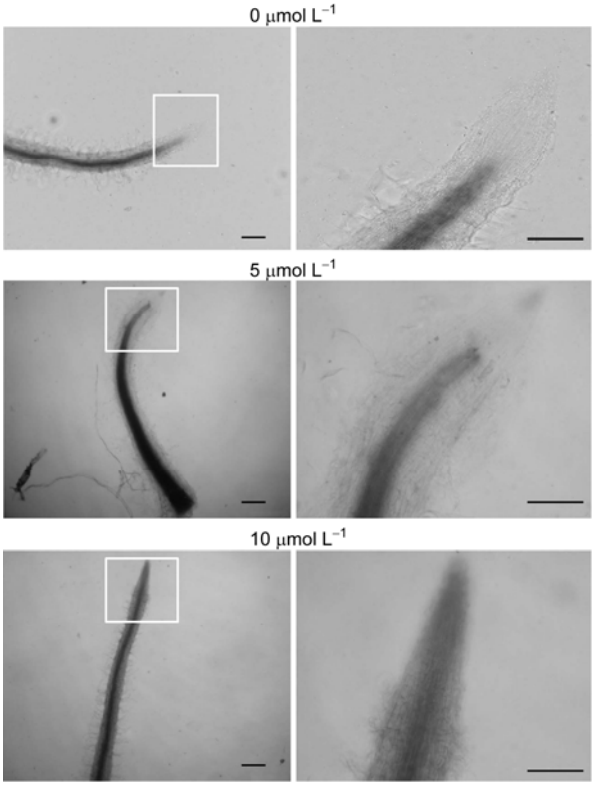

Figure 5 Cytokinin 6-BA induces transcription from the *MtAnn3* promoter. On the right are enlargements of the panels on the left. The bar indicates 50 μm.

either four or eight times in the different annexins [6]. In this study, we identified a novel annexin gene, *MtAnn3*, from *Medicago* plants. The MtAnn3 protein is composed of 92 amino acids and exhibits strong similarity to previously identified annexins. However, MtAnn3 contains only one repeat at the conserved C-terminal core domain, and it lacks a head domain. Transient expression in onion cells revealed the ability, shared with other annexins, to bind the plant cell membrane. Because the core domain mediates membrane binding, the reduced number of repeats in the core domain may account for the fact that the MtAnn3 proteins were not exclusively bound to cell membranes, but were also present in the cytoplasm.

M. truncatula responds to a critical bacterial signal, the Nod factor, which induces a rapid influx of Ca^{2+} in the root hair cells, which is immediately followed by membrane depolarization and root hair deformation [3]. With the aid of functional genetic and proteomic techniques, and using a whole-genome approach, a number of differentially expressed genes have been isolated from nodules and rhizobium-infected root hairs [15–17]. Among them, the calcium-dependent protein, calmodulin, calmodulin-binding protein and calcium-dependent protein kinase, participate in signaling transduction events. In two other separate studies, members of the calmodulin-dependent protein kinase family were shown to be directly involved in regulating the process of nodulation [18,19]. The annexin genes, *MtAnn1* and *MtAnn2*, were shown to be activated by the Nod factor during early stages of nodulation in *Medicago truncatula* [7,8]. Promoter-GUS fusion experiments suggest a similar pattern of *MtAnn3* expression in nodule primordia and young nodules. With our finding that the overexpression of *MtAnn3* in roots leads to root hair deformation in Ca^{2+}-free medium, we infer that MtAnn3 plays an important role in nodule formation. The results of this study are consistent with our previous findings that *MtAnn3* is upregulated in *nifA* mutant nodules and that a *nifA* mutant strain produces a super nodulation phenotype in *M. truncatula* [9].

Phytohormones have been shown to control nodule initiation and development. Brassinosteroids, methyl jasmonate, abscisic acid and ethylene negatively regulate nodule formation [20–23]. However, exogenous application of cytokinin to legume roots induces responses similar to those to the rhizobial Nod factors, including cortical cell division, amyloplast deposition and induction of early nodulin gene expression [24,25]. RNA interference of the cytokinin receptor homolog Cytokinin Response1 (*MtCRE1*) leads to cytokinin-insensitive roots, leading to a strong reduction in nodulation [26]. Cytokinin is the sole phytohormone studied thus far that has a positive role in nodule regulation. It is essential for nodule organogenesis and acts downstream of the Nod factor [27]. In our study, *MtAnn3* was induced by cytokinin. Further studies are needed to determine whether *MtAnn3* is involved in cytokinin-mediated signaling events during nodule organogenesis.

This work was supported by the National Natural Science Foundation of China (30770171) and the Shanghai Natural Science Foundation (05ZR14135).

1 Ishida T, Kurata T, Okada K, et al. A genetic regulatory network in the development of trichomes and root hairs. Annu Rev Plant Biol, 2008, 59: 365–861
2 Wymer C L, Bibikova T N, Gilroy S. Cytoplasmic free calcium distributions during the development of root hairs of *Arabidopsis thaliana*. Plant J, 1997, 12: 427–439
3 Ehrhardt D W, Wais R, Long S R. Calcium spiking in plant root hairs responding to *Rhizobium* nodulation signals. Cell, 1996, 85: 673-681
4 Cohn J, Day R B, Stacey G. Legume nodule organogenesis. Trends Plant Sci, 1998, 3: 105–110
5 Raynal P, Pollard H B. Annexins: The problem of assessing the biological role for a gene family of multifunctional calcium- and phospholipid-binding proteins. Biochim Biophys Acta, 1994, 1197: 63–93
6 Konopka-Postupolska D. Annexins: Putative linkers in dynamic membrane-cytoskeleton interactions in plant cells. Protoplasma, 2007, 230: 203–215
7 Niebel Fde C, Lescure N, Cullimore J V, et al. The *Medicago truncatula MtAnn1* gene encoding an annexin is induced by Nod factors and during the symbiotic interaction with *Rhizobium meliloti*. Mol Plant Microbe Interact, 1998, 11: 504–513
8 Manthey K, Krajinski F, Hohnjec N, et al. Transcriptome profiling in root nodules and arbuscular mycorrhiza identifies a collection of novel genes induced during *Medicago truncatula* root endosymbioses. Mol Plant Microbe Interact, 2004, 17: 1063–1077
9 Chen X T, Zou H S, Yao Z H, et al. *Sinorhizobium meliloti nifA* gene

exerts a pleiotropic effect on nodulation through the enhanced plant defense response. Chin Sci Bull, 2007, 52: 2925–2929
10 Tian Z X, Zou H S, Li J, et al. Transcriptome analysis of *Sinorhizobium meliloti* nodule bacteria in *nifA* mutant background. Chin Sci Bull, 2006, 51: 2079–2086
11 Liu Y, Zhu J B, Yu G Q, et al. The enoyl-ACP reductase gene, *fabI1*, of *Sinorhizobium meliloti* is involved in salt tolerance, swarming mobility and nodulation efficiency. Chin Sci Bull, 2010, 55: 259–262
12 Yao Z H, Tian Z X, Dai X M, et al. Complementation analyses of *Sinorhizobium meliloti nifA* mutant with different originated *nifA* genes. Chin Sci Bull, 2006, 51: 2748–2754
13 Gong Z Y, He Z S, Zhu J B, et al. *Sinorhizobium meliloti nifA* mutant induces different gene expression profile from wild type in Alfalfa nodules. Cell Res, 2006,16: 818–829
14 Limpens E, Ramos J, Franken C, et al. RNA interference in *Agrobacterium rhizogenes* transformed roots of *Arabidopsis* and *Medicago truncatula*. J Exp Bot, 2004, 55: 983–992
15 Covitz P A, Smith L S, Long S A. Expressed sequence tags from a root-hair-enriched *Medicago truncatula* cDNA library. Plant Physiol, 1998, 117: 1325–1332
16 Györgyey J, Vaubert D, Jiménez-Zurdo J I, et al. Analysis of *Medicago truncatula* nodule expressed sequence tags. Mol Plant Microbe Interact, 2000, 13: 62–71
17 Larrainzar E, Wienkoop S, Weckwerth W, et al. *Medicago truncatula* root nodule proteome analysis reveals differential plant and bacteroid responses to drought stress. Plant Physiol, 2007, 144: 1495–1507
18 Lévy J, Bres C, Geurts R, et al. A putative Ca^{2+} and calmodulin-dependent protein kinase required for bacterial and fungal symbioses. Science, 2004, 303: 1361–1364
19 Gargantini P R, Gonzalez-Rizzo S, Chinchilla D, et al. A CDPK isoform participates in the regulation of nodule number in *Medicago truncatula.* Plant J, 2006, 48: 843–856
20 Ligero F, Lluch C, Olivares J. Evolution of ethylene from roots of *Medicago sativa* plants inoculated with *Rhizobium meliloti*. J Plant Physiol, 1986, 125: 361–365
21 Nakagawa T, Kawaguchi M. Shoot-applied MeJA suppresses root nodulation in *Lotus japonicu*s. Plant Cell Physiol, 2006, 47: 176–180
22 Suzuki A, Akune M, Kogiso M, et al. Control of nodule number by the phytohormone abscisic acid in the roots of two legume species. Plant Cell Physiol, 2004, 45: 914–922
23 Terakado J, Fujihara S, Goto S, et al. Systemic effect of a brassinosteroid on root nodule formation in soybean as revealed by the application of brassinolide and brassinazole. Soil Sci Plant Nutr, 2005, 51: 389–395
24 Bauer P, Ratet P, Crespi M, et al. Nod factors and cytokinins induce similar cortical cell division, amyloplast deposition and Msenod12A expression patterns in *alfalfa* roots. Plant J, 1996, 10: 91–105
25 Lorteau M A, Ferguson B J, Guinel F C. Effects of cytokinin on ethylene production and nodulation in pea (*Pisum sativum*) cv. *Sparkle*. Physiol Plant, 2001, 112: 421–442
26 Gonzalez-Rizzo S, Crespi M, Frugier F. The *Medicago truncatula CRE1* cytokinin receptor regulates lateral root development and early symbiotic interaction with *Sinorhizobium meliloti.* Plant Cell, 2006, 18: 2680–2693
27 Frugier F, Kosuta S, MurrayJ D, et al. Cytokinin: Secret agent of symbiosis. Trends Plant Sci, 2008, 13: 115–120